



# Influence of water vapor on long-term performance and accelerated degradation of solid oxide fuel cell cathodes

R.R. Liu<sup>a,1</sup>, S.H. Kim<sup>a</sup>, S. Taniguchi<sup>b</sup>, T. Oshima<sup>a</sup>, Y. Shiratori<sup>a</sup>, K. Ito<sup>a,b</sup>, K. Sasaki<sup>a,b,\*</sup>

<sup>a</sup> Kyushu University, Department of Hydrogen Energy Systems, Faculty of Engineering, Motoooka 744, Nishi-ku, Fukuoka 819-0395, Japan

<sup>b</sup> International Research Center for Hydrogen Energy, Motoooka 744, Nishi-ku, Fukuoka 819-0395, Japan

## ARTICLE INFO

### Article history:

Received 26 June 2010

Received in revised form 4 August 2010

Accepted 10 August 2010

Available online 18 August 2010

### Keywords:

Cathode

SOFC

Durability

Degradation

Water vapor

## ABSTRACT

The influence of water vapor in the air on the performance and durability of solid oxide fuel cell (SOFC) has been investigated for the state-of-the-art cathodes,  $(\text{La}_{0.8}\text{Sr}_{0.2})_{0.98}\text{MnO}_3$  (LSM) and  $\text{La}_{0.6}\text{Sr}_{0.4}\text{Co}_{0.2}\text{Fe}_{0.8}\text{O}_3$  (LSCF). Durability experiments were carried out at 800 °C up to 1000 h with various water vapor containing-air fed to the cathode side. Both types of cathode materials were basically stable under typical water vapor concentrations in the ambient air. Degradations could be accelerated at much higher water vapor concentrations, which could be associated with the decomposition of the cathode materials. Temperature dependence of this degradation was analyzed between 700 °C and 900 °C under 10 vol% water vapor concentration, which showed that the effect of water vapor depends strongly on the temperature and led to a severe degradation at 700 °C within a short time period for both cathode materials.

© 2010 Elsevier B.V. All rights reserved.

## 1. Introduction

Solid oxide fuel cell (SOFC) is regarded as an energy device with several advantages, such as high electrical efficiencies, low-emission of  $\text{SO}_x$  and  $\text{NO}_x$  and possibility of internal reforming. SOFC is expected to be used as a practical energy system for co-generation, distributed power generation and transportation applications [1–3]. Various degradation mechanisms, however, may appear such as chemical instability between different components of cells and sintering of electrode materials especially during a long-range operation at high temperatures. Improvement of long-term stability of SOFC is one of the major issues of this technology and research efforts are being made to clarify the mechanisms of cell performance degradation and to improve durability effectively.

There are various impurities contained in the gas supplied to cells which could lower the SOFC performance. Influence of  $\text{H}_2\text{S}$ , which is a major impurity in hydrocarbon based fuels, on the anode performance has been discussed so far [4]. As for the cathode, humidification effect has been investigated and it was reported that nano-sized particles appeared between the LSM/YSZ interface [5]. Yet very limited information has been obtained about the influence

of humidity, on the cathode performance especially with respect to the long-term durability of SOFCs.

Here we are focusing on the degradation by water vapor with respect to concentration and operating temperature, on the performance and durability of SOFC cathodes. Changes in electrode performance and cathode microstructure and composition by the effect was studied and analyzed to reveal the degradation mechanism of LSM and LSCF based cathodes.

## 2. Experimental procedures

Electrolyte-supported cells are used in this study. Electrolyte plates made of 10 mol%  $\text{Sc}_2\text{O}_3$ –1 mol%  $\text{CeO}_2$ –89 mol%  $\text{ZrO}_2$  (abbreviated by ScSZ, Daiichi Kigenso Kagaku Kogyo) with the thickness of 200  $\mu\text{m}$  were selected. Mixture of 56 wt% NiO and 44 wt% ScSZ was used for the anode material. The cathodes in this study had double layer structures. Mixture of  $(\text{La}_{0.8}\text{Sr}_{0.2})_{0.98}\text{MnO}_3$  (LSM) (>99.9%, Praxair, CT, USA) and ScSZ with a weight ratio of 1:1 was applied as a functional layer (first layer), and coarse LSM powder (calcined at 1400 °C for 5 h and ball-milling 24 h) with the particle size of 10–20  $\mu\text{m}$  was used as a current collecting layer (second layer) for LSM cathode. The anode and LSM cathode layers were screen-printed on the electrolyte plates followed by sintering at 1300 °C for 3 h and at 1200 °C for 5 h, respectively.  $\text{La}_{0.6}\text{Sr}_{0.4}\text{Co}_{0.2}\text{Fe}_{0.8}\text{O}_3$  (LSCF) (>99.9%, Praxair, CT, USA) was used for LSCF cathode and it was sintered at 900 °C on the  $\text{Ce}_{0.9}\text{Gd}_{0.1}\text{O}_2$  (GDC) (>99.9%, Rhodia, Tokushima, Japan) layer which had been already sintered on the electrolyte plate at 1300 °C as a protecting layer. Electrode area was 8 mm × 8 mm and Pt mesh was used as the current collector.

\* Corresponding author at: International Research Center for Hydrogen Energy, Kyushu University, West-4, Room 628, Motoooka 744, Nishi-ku, Fukuoka 819-0395, Japan. Tel.: +81 92 802 3143; fax: +81 92 802 3223.

E-mail address: [sasaki@mech.kyushu-u.ac.jp](mailto:sasaki@mech.kyushu-u.ac.jp) (K. Sasaki).

<sup>1</sup> On leave from Faculty of Sciences, Chang Chun University, Wei Xing Road 6543, Chang Chun 130022, Jilin Province, China.

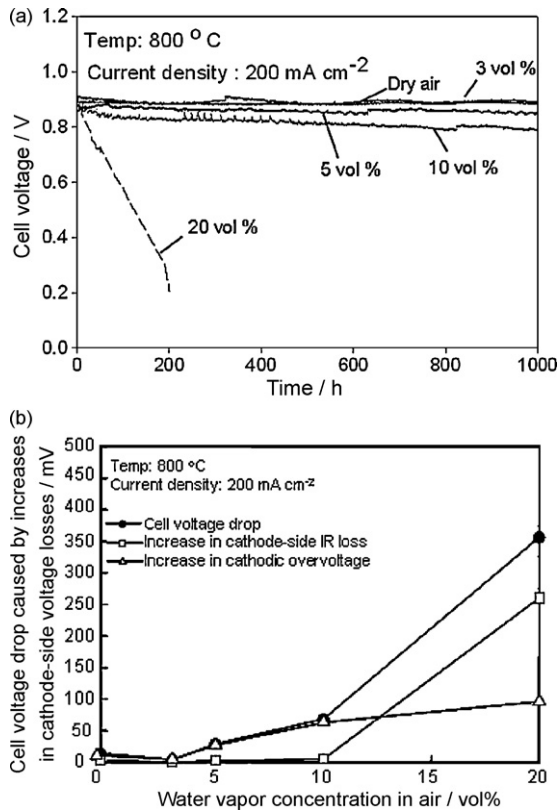


**Fig. 1.** (a) Cell voltage measured at 800 °C under the constant current density of 200 mA cm<sup>-2</sup> showing the influence of water vapor in air on the performance of LSM cathode; (b) cell voltage drop, increase in cathode-side IR loss, and increase in cathodic overvoltage during 200 h.

For electrochemical characterizations, 3 vol% humidified H<sub>2</sub> was supplied to the Ni-ScSZ anode, and humidified air (3, 5, 10 and 20 vol%) was supplied to the cathode to clarify the dependence of cell durability on water vapor concentration. Note that the saturated concentration of water vapor at room temperature is ca. 3 vol% and these experiments at higher water vapor concentrations were conducted as acceleration tests to understand degradation phenomena. Cell voltages under open circuit condition and under a constant current density of 200 mA cm<sup>-2</sup> were measured for 1000 h at 800 °C. In order to clarify the dependency of operating temperature on cell performance, experiments were conducted between 700 °C and 900 °C up to 200 h with 10 vol% humidified air supplied to the cathode. During experiments, cathode-side IR loss

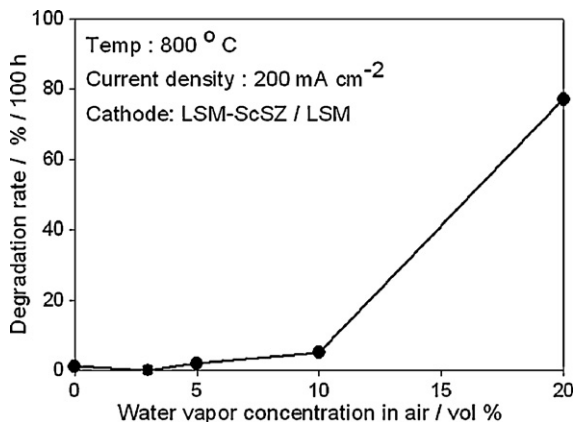


**Fig. 2.** Influence of water vapor in air on the degradation rate of the cell with LSM cathode within 200 h.

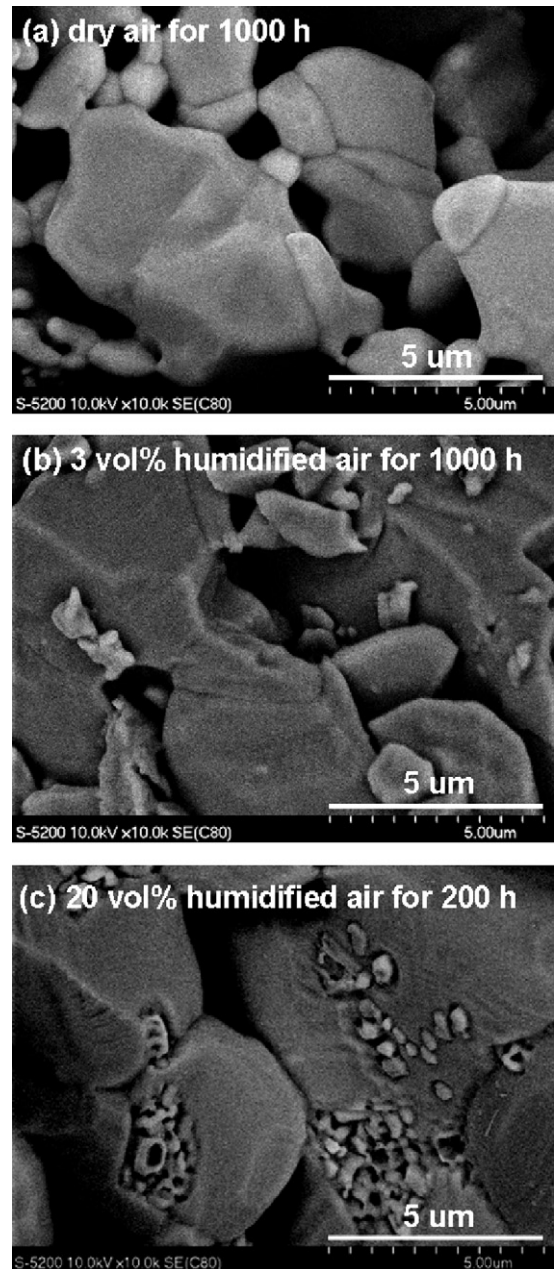


**Fig. 3.** FESEM images of LSM particles in the current collecting layer after operation in (a) dry air for 1000 h, (b) 3 vol% humidified air for 1000 h, and (c) 20 vol% humidified air for 200 h, at 800 °C.

and cathodic polarization were measured by the current interrupt method to detect the major origin of cell voltage degradation.

FESEM-EDX (Field Emission Scanning Electron Microscope-Energy Dispersive X-ray analysis, S-5200, Hitachi), STEM-EDX (Scanning Transmission Electron Microscope, HD-2300A, Hitachi) and X-ray diffraction (XRD with Cu K $\alpha$  radiation) (Rigaku RINT Ultima III, Japan) were applied to investigate changes in cathode microstructure and composition after cell performance tests.

### 3. Results and discussion

#### 3.1. Dependency of cell performance and durability on water vapor concentration

##### 3.1.1. LSM cathode

Fig. 1 shows the influence of water vapor on cell performance with the LSM cathode. Dependency of cell voltage on water vapor

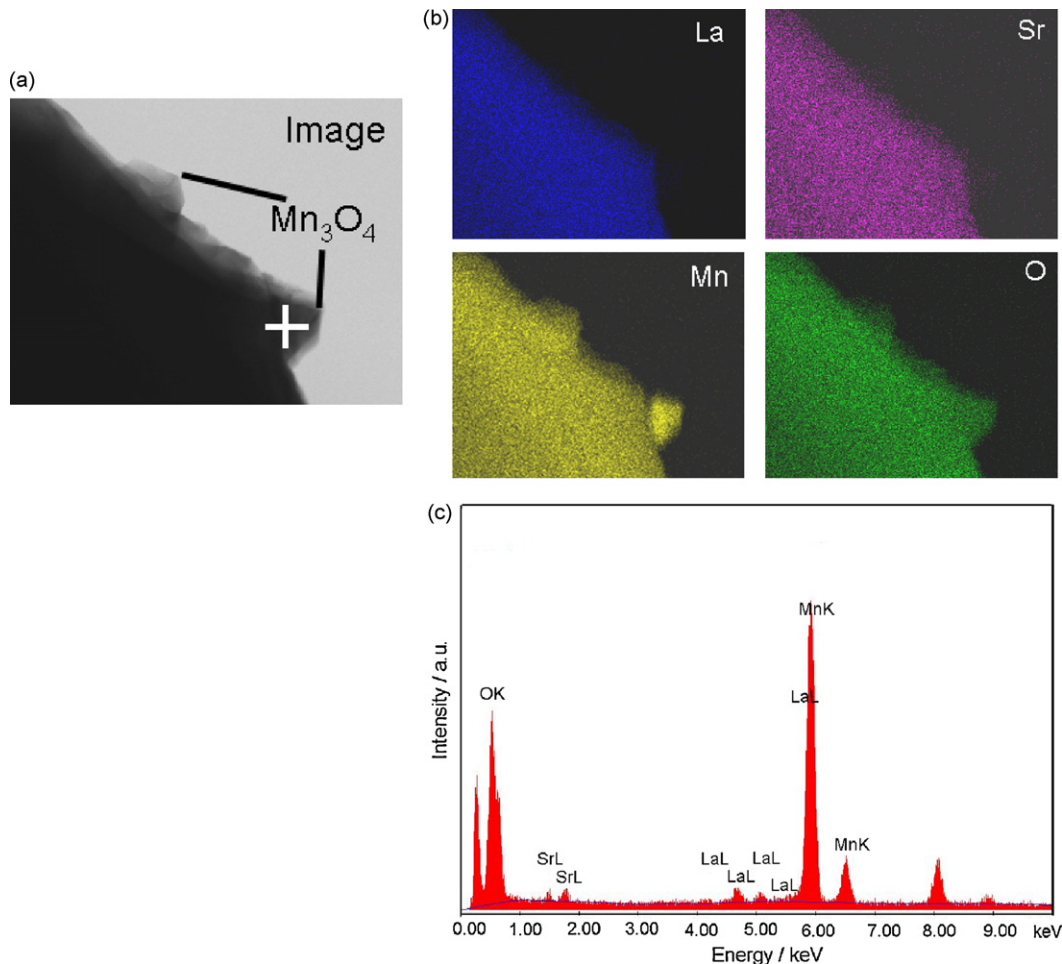


**Fig. 4.** (a) STEM image and (b) EDX results of  $\text{Mn}_3\text{O}_4$  particle appeared in the current collecting layer of LSM after operation in 20 vol% humidified air for 200 h at  $800^\circ\text{C}$ . The EDX spectrum of the cross point is shown in (c).

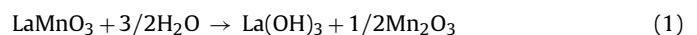
concentration at  $800^\circ\text{C}$  over 1000 h was shown in Fig. 1(a). Fig. 1(b) shows the change in cell voltage drop, cathode-side IR loss, and cathodic polarization over 200 h. Furthermore, the degradation rate of cell voltage per 100 h was calculated, as shown in Fig. 2. These results demonstrated that gradual degradation at 10 vol% of water vapor was accompanied by an increase in cathodic overvoltage and rapid degradation for 20 vol% humidified air was caused predominately by an increase in cathode-side IR loss (Fig. 1(b)). Under the typical operational conditions with dry, 3 and 5 vol% humidified air, degradation rate was smaller. Especially, 3 vol% humidified air even minimized the voltage drop. Indeed, Sakai et al. reported that cathode performance in feeding 3 vol% humidified air was better than that in feeding dry air because of the promotion of the surface exchange reactions [6]. A slight change in the cathode microstructure was observed, however, even in the case of 3 vol% humidified air after 1000 h operation as mentioned below.

Fig. 3 shows the surface morphology of the LSM particles in the current collecting layer, observed by FESEM. For the dry air (Fig. 3(a)), even after 1000 h operation, LSM particle had a smooth surface and still maintained the initial morphology. For the case of 3 vol% humidified air, there are some changes in morphology but not obvious, that is some finer particles appeared between LSM particles (Fig. 3(b)). After 200 h of operation in 20 vol% humidified air (Fig. 3(c)), however, plenty of segregates (100 nm in size) appeared on the surface of LSM. The segregated particles were quantitatively analyzed by STEM-EDX and identified as manganese oxide in which the ratio of Mn and O was about 2.8:3.9 as shown in Fig. 4. At the

same time, XRD result showed the existence of  $\text{Mn}_2\text{O}_3$  and  $\text{Mn}_3\text{O}_4$  after exposing to 20 vol% humidified air as shown in Fig. 5. Furthermore, in the first layer of the LSM cathode, Pt particles were observed at the interface between LSM and ScSZ, namely three phase boundaries (TPB), as reported previously [7].

Deviation of LSM composition from  $(\text{La}_{0.8}\text{Sr}_{0.2})_{0.98}\text{MnO}_3$  may occur especially near the surface resulting in lowering electrical connection between the adjacent LSM particles. This may be the main reason of the rapid degradation accompanied by the cathode-side IR loss. Formation of  $\text{Mn}_3\text{O}_4$  in LSM cathode was observed under electrochemical current load [8], and its segregation on the surface of dense LSM under steep oxygen potential gradients [9] has been reported. Similar reactions between LSM and water vapor may occur and it explains the formation of  $\text{Mn}_3\text{O}_4$  in this study. We have also reported the fact that  $\text{La}_2\text{O}_3$  segregation was clearly observed on LSM surface under 40 vol% humidified air condition at  $800^\circ\text{C}$  [10].

A possible degradation mechanism of LSM at very high water vapor concentrations is schematically shown in Fig. 6. Fig. 6(a) illustrates the decomposition of LSM by water vapor to  $\text{Mn}_2\text{O}_3$  and  $\text{La}(\text{OH})_3$  on the surface of LSM, which is described in Eq. (1):



$\text{La}(\text{OH})_3$  is not stable so that it may decompose to  $\text{La}_2\text{O}_3$  and  $\text{H}_2\text{O}$  as shown in Eq. (2).

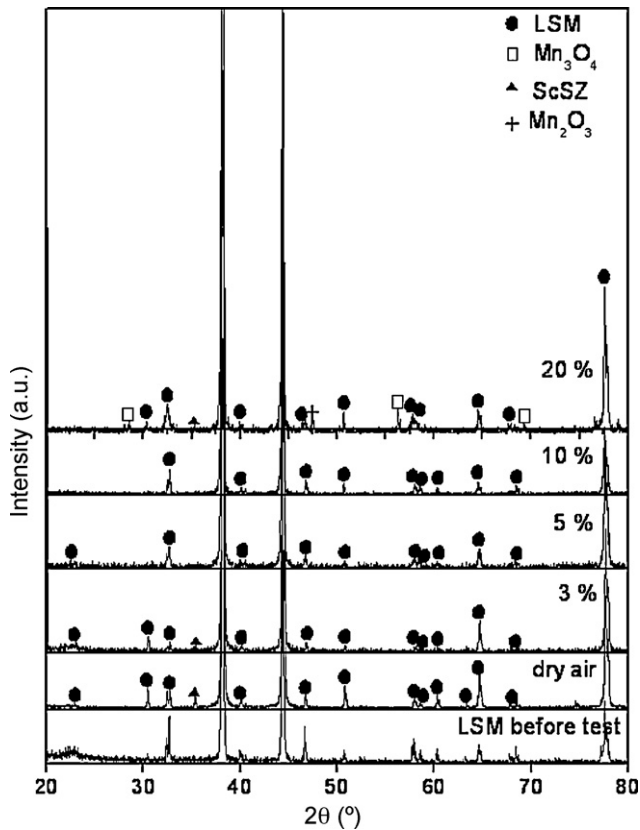


Fig. 5. XRD patterns of LSM cathodes before and after cell tests under different water vapor concentrations.

As a result, water vapor acted as a catalyst to promote the decomposition of perovskite LSM cathode to form  $Mn_2O_3$  and  $La_2O_3$  and led to the fatal degradation of cell performance. The formation of  $Mn_3O_4$  observed by STEM-EDX shown in Fig. 4 may be due to the reduction of  $Mn_2O_3$  under operating conditions.

Xiong et al. have reported that  $PtO_2$  vaporized from Pt mesh or Pt wire used for current collection and it was deposited as metallic Pt at the triple phase boundary, where oxygen partial pressure becomes locally quite low under a high cathodic overvoltage [11]. The deposition of Pt observed in this study suggests that higher concentration of water vapor might therefore accelerate such Pt evaporation/deposition processes. Fig. 6(b) shows the deposition mechanism of Pt at the TPB sublimated from the platinum mesh (or lead wire) which was used as a current collector. These phenomena, however, may not be the most predominant mechanism for the cathode performance degradation by water vapor.

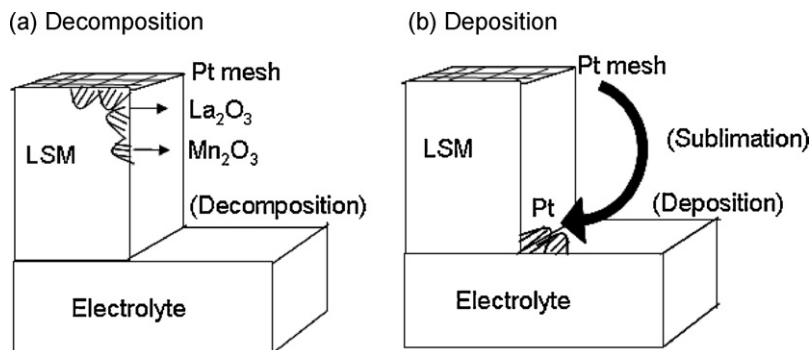


Fig. 6. Degradation mechanisms at very high water vapor concentrations for LSM cathodes.

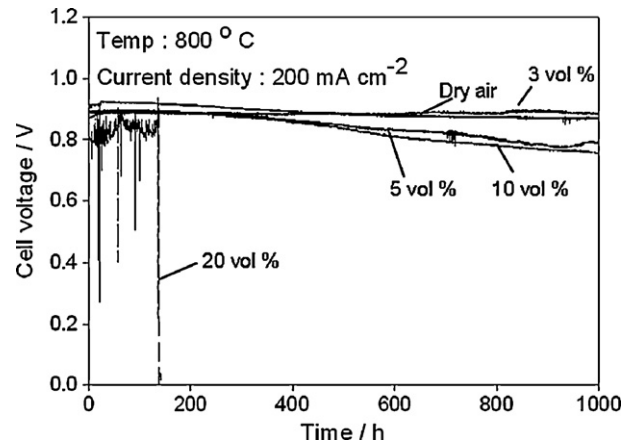


Fig. 7. Cell voltage measured at 800 °C under the constant current density of 200 mA cm<sup>-2</sup> showing the influence of water vapor in air on the performance of the cell with the LSCF cathode.

### 3.1.2. LSCF cathode

Fig. 7 shows the influence of water vapor on the performance of the LSCF cathode. Degradation rate was rather small as shown in Fig. 8, compared to the LSM cathode (see Fig. 2) within 200 h. But degradation occurred more rapidly than LSM after 400 h, suggesting that LSCF has poorer stability under such humidified air conditions for long-term operation. For the case of 20 vol% water vapor, the cell with the LSCF cannot work over 200 h due to the detachment of the LSCF cathode layer from the GDC interlayer.

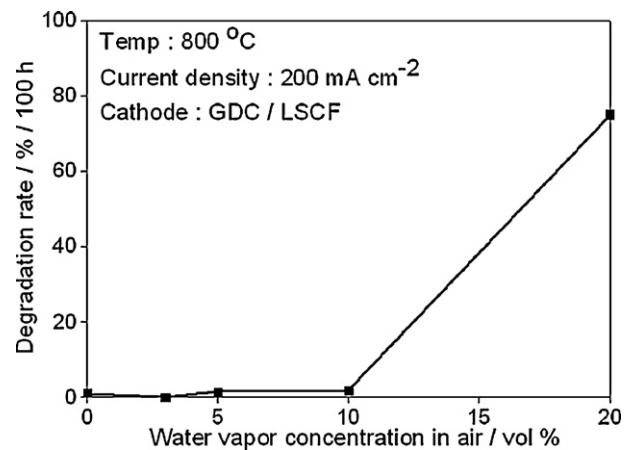
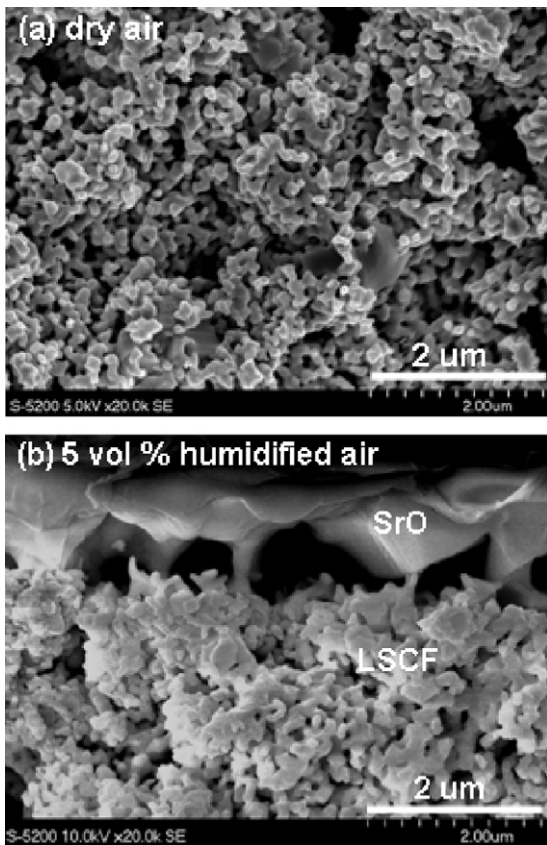


Fig. 8. Degradation rate of cell voltage measured at 800 °C by 200 h under the constant current density of 200 mA cm<sup>-2</sup> showing the influence of water vapor in air on the performance of the cell with LSCF cathode.



**Fig. 9.** FESEM micrographs of the LSCF surface, after 1000 h test at 800 °C shown in Fig. 5, operated with different cathode gases: (a) dry air and (b) 5 vol% humidified air.

The morphological change of the LSCF cathode by the 1000 h of operation under 200 mA cm<sup>-2</sup> at 800 °C was observed. As shown in Fig. 9(a), LSCF particles show a regular appearance. The presence of a layer enriched in Sr (probably SrO) on the surface of the LSCF cathode in 5 vol% humidified air (see Fig. 9(b)) would be the major origin

of the observed degradation. Besides, the formation of Fe enrichment was observed on the LSCF cathode surface by FESEM-EDX as shown in Fig. 10, which resulted from the decomposition of the LSCF cathode material. Although the perovskite structure observed by XRD has not been destroyed, it may influence the electrochemical activity and the thermal expansion coefficient of LSCF which strongly depends on Sr content, and finally result in the degradation of cell performance.

At lower humidified air conditions (~3 vol%) a slight degradation was observed accompanied with slight change in cathode microstructure, which implied possibility of increasing degradation after longer term operation. Degradation mechanism was the same as higher humidified air. Thus, cell tests under higher humidified conditions can be regarded as “accelerated experiments” for long-term operation under lower humidified conditions.

### 3.2. Temperature dependence of cathode degradation effect by water vapor

#### 3.2.1. LSM cathode

From the above results, 10 vol% humidified air was selected to investigate the influence of operating temperature on the cathode degradation by water vapor. As shown in Fig. 11, cell performance degradation depended strongly on operating temperature. At 900 °C cell voltage remained almost the same during the test, except for an initial increase in cell voltage. Slight degradation can be seen at 800 °C. At 700 °C, cell test was not able to continue over 50 h because of a drastic increase in both cathodic polarization and cathode-side IR loss.

FESEM images of cross section of the LSM cathode after the cell tests at different temperatures are shown in Fig. 12. In the case of 900 °C, LSM and ScSZ particles are in regular arrangement and well networked, which ensure the good electrical contact and sufficient electrochemical reactions. For the case of 800 °C, although some finer particle appeared, marked morphology change did not appear as shown in Fig. 12(b), corresponding to a slight degradation of cell performance (see Fig. 1). Significant morphology change was observed in the first layer of the cathode operated at 700 °C (Fig. 12(c)), and plenty of finer particles appeared in the LSM. This morphology change would affect the electrical property and lead to the serious degradation of cell performance as shown in Fig. 11.

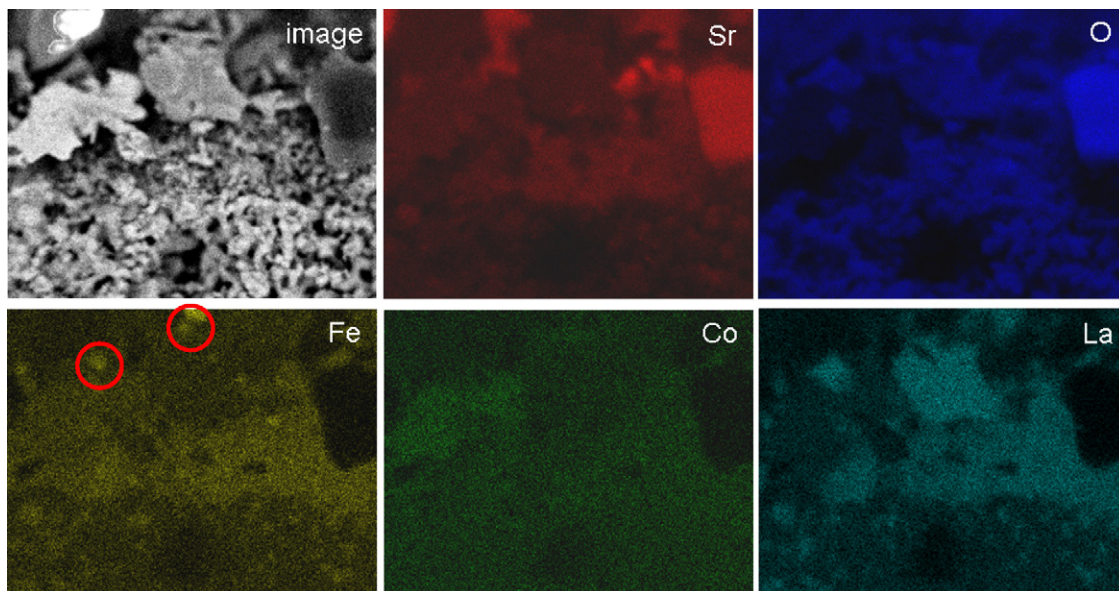


**Fig. 10.** FESEM image and EDX results of Sr and Fe enrichment appeared on the surface of LSCF after operation in 5 vol% humidified air for 1000 h at 800 °C.

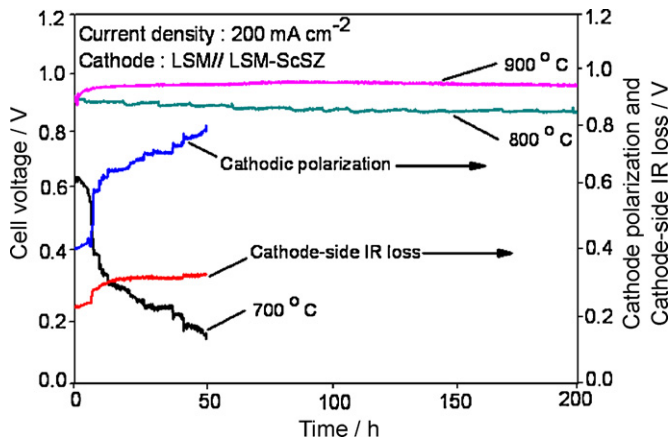


**Fig. 11.** Cell voltage measured under the constant current density of  $200 \text{ mA cm}^{-2}$  with 10 vol% humidified air supplied to LSM cathode at different temperature.

### 3.2.2. LSCF cathode

Similar results to the LSM cathode have been obtained for the LSCF cathode as shown in Fig. 13. Most serious degradation occurred at  $700^\circ\text{C}$  in a short time period, accompanied by a considerable increase in cathode-side IR loss and cathodic polarization when 10 vol% humidified air was fed to the LSCF cathode. Cell voltage drops were negligible for the other two cases of 900 and  $800^\circ\text{C}$ .

From the FESEM images of LSCF surface after the cell tests shown in Fig. 14, it was found that cathode morphology did not change significantly after the cell test at  $900^\circ\text{C}$ . For the case of  $800^\circ\text{C}$ , there

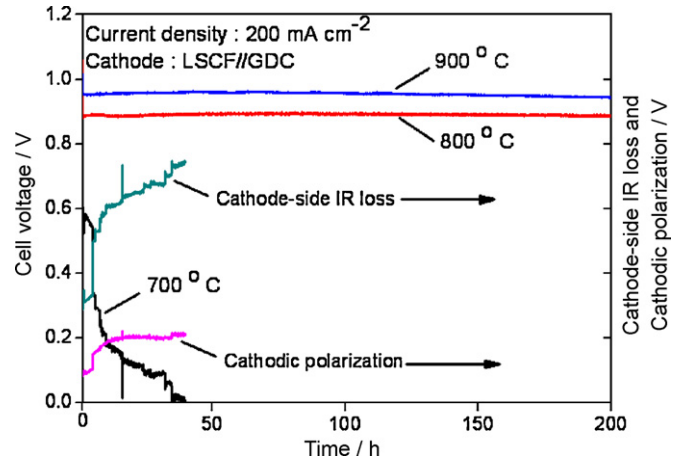


**Fig. 13.** Cell voltage measured under the constant current density of  $200 \text{ mA cm}^{-2}$  with 10 vol% humidified air supplied to LSCF cathode at different temperature. Cathodic polarization and cathode-side IR loss were also shown in this figure for the case of  $700^\circ\text{C}$ .

was no obvious change in cathode morphology, either. At  $700^\circ\text{C}$ , porosity of LSCF cathode was reduced after exposing to humidified air (Fig. 14(c)), which will hinder gas diffusion and lead to increase in cathodic polarization. Sr-rich oxide was also detected by EDX analysis which implied that decomposition of LSCF cathode material would be the main reason of rapid cell degradation observed at  $700^\circ\text{C}$ .

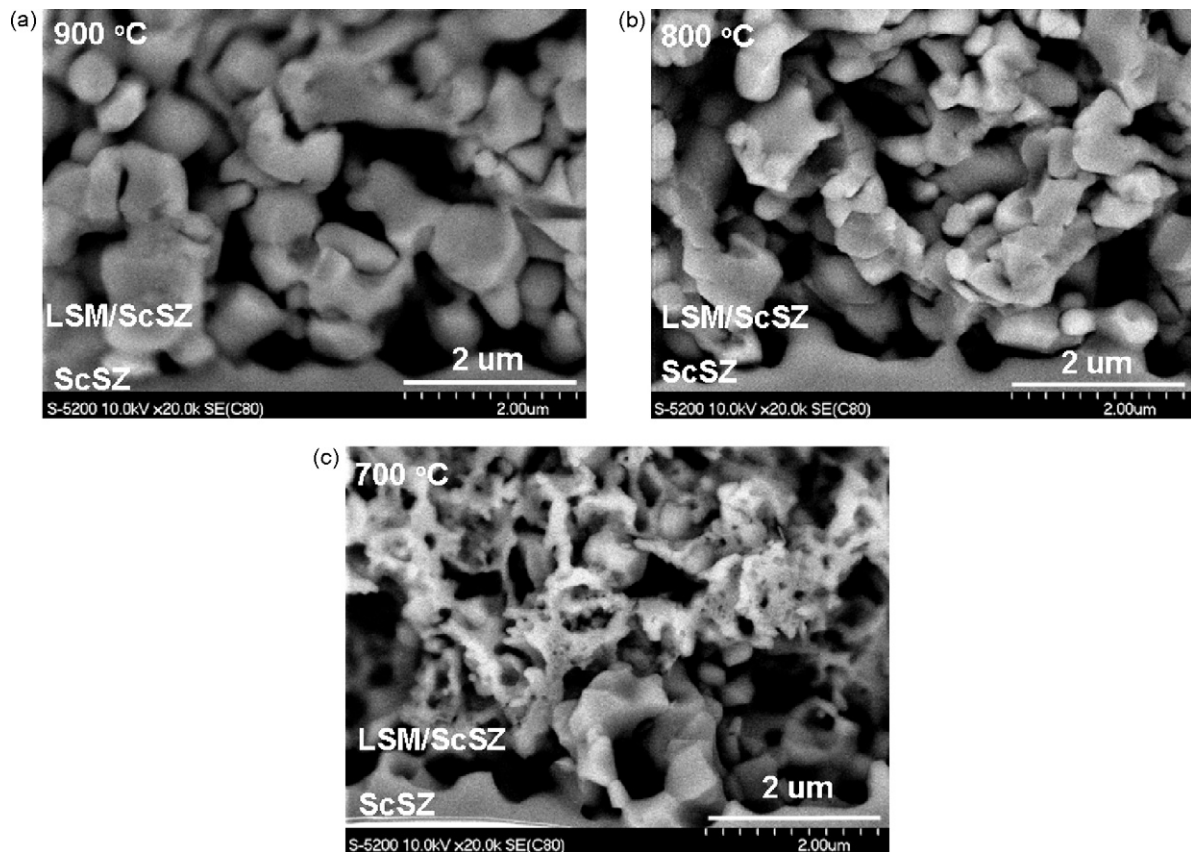


**Fig. 12.** FESEM micrographs of functional layer of LSM cathode after cell test operated at different temperatures: (a)  $900^\circ\text{C}$ , (b)  $800^\circ\text{C}$ , and (c)  $700^\circ\text{C}$ .

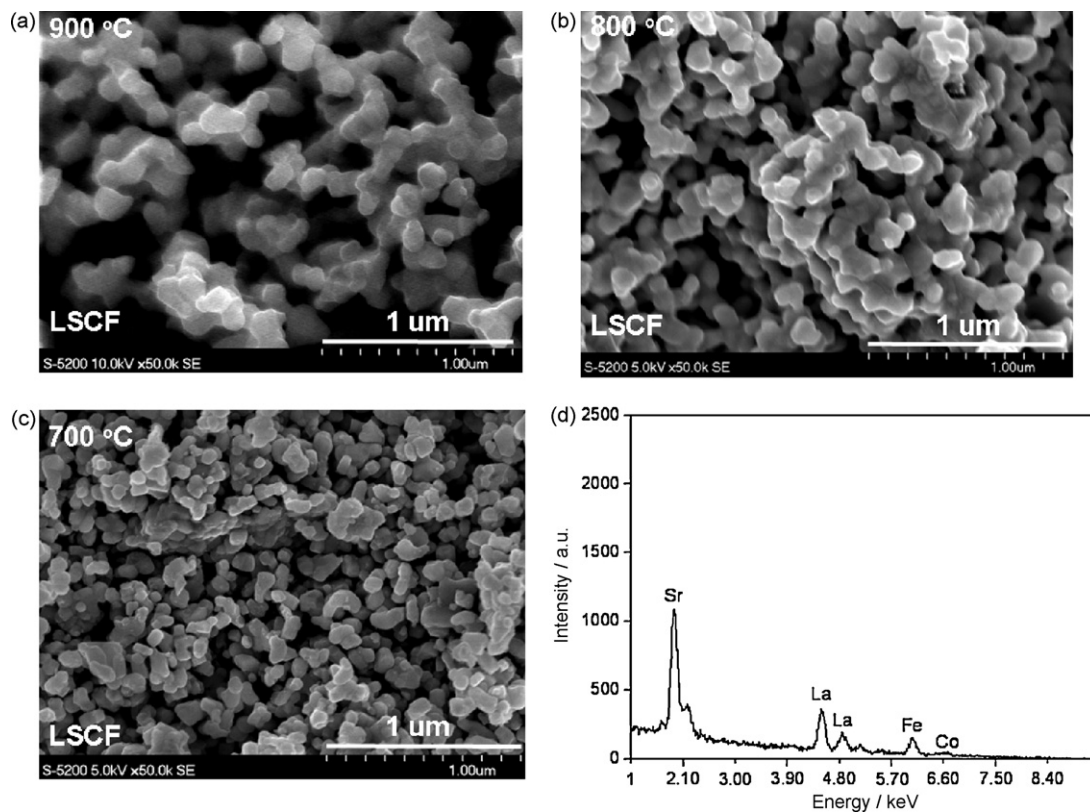


**Fig. 14.** FESEM micrographs and EDX spectra of LSCF surface after current passage at  $200 \text{ mA cm}^{-2}$  for 200 h in 10 vol% humidified air. (a–c) The surface image of the LSCF at  $900^\circ\text{C}$ ,  $800^\circ\text{C}$ , and  $700^\circ\text{C}$ , respectively. EDX spectra of cathode surface operated at  $700^\circ\text{C}$  are shown in (d).

#### 4. Conclusion

The influence of water vapor on cathode degradation depended strongly on its concentration and operating temperature. Higher concentration of water vapor at  $800^\circ\text{C}$  caused larger cell voltage drops, which was attributed to the increase in both cathodic overvoltage and cathode-side IR loss. This degradation mode was associated with decomposition of LSM to form  $\text{Mn}_3\text{O}_4$  segregates on the surface of LSM. LSCF showed relatively poorer tolerance to water vapor compared to LSM for long-term operation. Sr enrichment (and possible formation of SrO) on the surface of LSCF cathode may be related to the degradation phenomena. It is concluded that long-term degradation of LSM cathodes and LSCF cathodes by water vapor is caused mainly by gradual decomposition of the cathode materials on their surface, rather than a chemical reaction between the cathode and the electrolyte in the vicinity of three phase boundaries. Further, the lower the temperature becomes, the more serious degradation occurs accompanying by decomposition of these typical cathode materials.

#### Acknowledgments

This research was carried out partly with the financial support from the NEDO project “Development of System

and Elemental Technology of SOFC”, to which we gratefully acknowledged.

#### References

- [1] N.Q. Minh, T. Takahashi, *Science and Technology of Ceramic Fuel Cells*, Elsevier, Amsterdam, 1995.
- [2] H. Yokokawa, N. Sakai, in: W. Vielstich, Lamm, H.A. Gasteiger (Eds.), *Handbook of Fuel Cell Fundamental Technology and Application*, vol. 1, John Wiley & Sons, 2003, pp. 219–266.
- [3] S.C. Singhal, *Solid Oxide Fuel Cells VI*, PV 99–19, The Electrochemical Society, Pennington, JU, USA, 1999, p. 39.
- [4] K. Sasaki, S. Adachi, K. Haga, M. Uchikawa, J. Yamamoto, A. Iyoshi, J.T. Chou, Y. Shiratori, K. Ito, *ECS Trans.* 7 (1) (2007) 1675.
- [5] J. Nielsen, A. Hagen, Y.L. Liu, *Solid State Ionics* 181 (2010) 517–524.
- [6] N. Sakai, K. Yamaji, T. Horita, Y. Xiong, H. Kishimoto, H. Yokokawa, *J. Electrochem. Soc.* 150 (6) (2003) A689.
- [7] R.R. Liu, S.H. Kim, Y. Shiratori, T. Oshima, K. Ito, K. Sasaki, *ECS Trans.* 25 (2) (2009) 2859.
- [8] S.P. Jiang, W. Wang, *Solid State Ionics* 176 (2005) 1185.
- [9] H. Nishiyama, M. Aizawa, H. Yokokawa, T. Horita, N. Sakai, M. Dokiya, *J. Electrochem. Soc.* 143 (7) (1996) 2332.
- [10] S.H. Kim, K.B. Shim, C.S. Kim, J.T. Chou, T. Oshima, Y. Shiratori, K. Ito, K. Sasaki, *J. Fuel Cell Sci. Technol.* 7 (2) (2010) 21011.
- [11] Y. Xiong, K. Yamaji, H. Kishimoto, M.E. Brito, T. Horita, H. Yokokawa, *Electrochem. Solid State Lett.* 12 (3) (2009) B31.